ACSNANO
www.acsnano.org
ARTICLE

Paper-Based Triboelectric Nanogenerators Made of Stretchable Interlocking Kirigami Patterns

Changsheng Wu,[†,‡] Xin Wang,[†,‡] Long Lin,[†] Hengyu Guo,[†] and Zhong Lin Wang[*,†,§]

[†]School of Materials Science and Engineering, Georgia Institute of Technology, Atlanta, Georgia 30332-0245, United States

[§]Beijing Institute of Nanoenergy and Nanosystems, Chinese Academy of Sciences, National Center for Nanoscience and Technology (NCNST), Beijing 100083, P. R. China

Supporting Information

ABSTRACT: The development of stretchable energy generation devices is indispensable for achieving stretchable, self-powered electronic systems. In this paper, a type of highly stretchable triboelectric nanogenerators made from conventional, inelastic materials such as paper is presented. It exploits a rationally designed interlocking kirigami structure and is capable of harvesting energy from various types of motions such as stretching, pressing, and twisting owing to the shape-adaptive thin film design. Energy harvested from the as-fabricated devices has been used for powering an LCD screen and lighting LED arrays. Furthermore, the paper-based devices have also been demonstrated for self-powered acceleration sensing and self-powered sensing of book opening and closing. This work introduces traditional kirigami into the development of stretchable triboelectric nanogenerators and verifies its promising applications in both power generation and self-powered sensing.

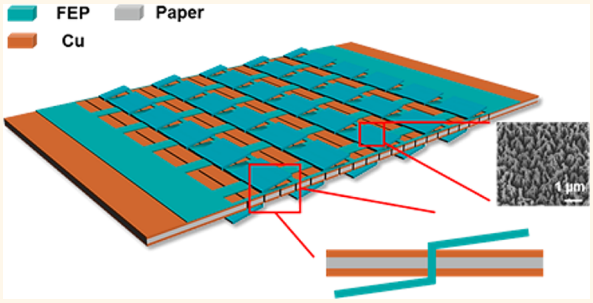

KEYWORDS: *triboelectric nanogenerators, stretchable electronics, stretchable power sources, self-powered sensors, kirigami*

Over the past decade, flexible and stretchable electronics has emerged as the next-generation of functional devices and has attracted extensive interests from both academia and industry. Compared to its rigid counterparts, flexible and stretchable electronics offers great deformability without sacrificing the device's performance and reliability and thus has promising applications in wearable devices, epidermal electronics, implantable devices, *etc.*[1−5] Efforts have also been devoted to deformable energy storage devices,[6] such as thin-film-based bendable supercapacitors and batteries,[7−10] stretchable supercapacitors using carbon-nanotube-coated textiles,[11] and stretchable lithium-ion batteries using serpentine interconnects.[12] However, the development of stretchable energy generation devices has the great potential of evolving existing stretchable electronics into a higher level of stretchable self-powered electronic systems and thus deserves more attention.

Mechanical energy is a ubiquitous energy source and has long been used for electricity generation through electromagnetic generators and later through piezoelectric and triboelectric nanogenerators (TENGs). Among them, TENGs, which convert mechanical energy into electricity using the coupling effects between triboelectrification and electrostatic induction, have the advantages of low cost and abundant material choices and thus are highly promising in offering stretchable energy generation solutions for stretchable electronics.[13−17] Yang *et al.* have reported the fabrication of a stretchable TENG using serpentine-patterned electrodes and a wavy-structured Kapton film, achieving a maximum tensile strain of 22%.[18] Yi *et al.* also has devised a partially stretchable TENG using rubber and an aluminum film, where the rubber part is highly stretchable.[19] However, the stretchability of these TENGs are highly dependent on their constituent materials, and materials with intrinsic elasticity like PDMS and rubber are necessary.[18−20] This greatly weakens the material advantage of TENGs over other energy generation technologies, and thus, methods of introducing stretchability from designed structures rather than materials are meaningful. One promising approach is taking use of traditional origami or kirigami patterns, which have been proven to be successful in fabricating elastic nanocomposites,[21] solar trackers,[22] deformable lithium batteries,[23] reprogrammable mechanical metamaterials,[24] and optical devices.[25] Recently Yang *et al.* demonstrated the use of origami configurations to achieve stacked TENGs without

Received: February 5, 2016
Accepted: April 8, 2016

DOI: 10.1021/acsnano.6b00949
ACS Nano XXXX, XXX, XXX−XXX

expanding the area or complicating the fabrication process, but their design was too bulky and not rigid enough for ideal stretchable power sources.[26]

Therefore, our research here focuses on introducing a type of highly stretchable TENGs by using the traditional kirigami patterns, whose stretchability originates from the designed structures instead of constituent materials. The proposed method enables stretchable TENGs to be made from materials without intrinsic stretchability, such as paper, fluorinated ethylene propylene (FEP), polytetrafluoroethylene (PTFE), poly(ethylene terephthalate) (PET), and Kapton and, thus, is very versatile. The fabricated devices sustained an ultrahigh tensile strain up to 100% and were capable of harvesting energy from various types of motions such as stretching, pressing and twisting. Simple hand clapping on the device could generate a maximum open-circuit voltage of 115.49 V and a maximum transferred charge quantity of 39.87 nC. Furthermore, the KTENG has been demonstrated for a broad range of applications, such as powering a LCD screen, lighting LED arrays, self-powered acceleration sensing, and self-powered sensing of book opening and closing. This work presents the progress of stretchable TENGs for application in stretchable and flexible electronics, and it will shed light on future directions of kirigami-based devices.

RESULTS AND DISCUSSION

The schematic structure of the stretchable, paper-based TENG with interlocking kirigami patterns (KTENG) and related pictures are illustrated in Figure 1a. The KTENG consist of one

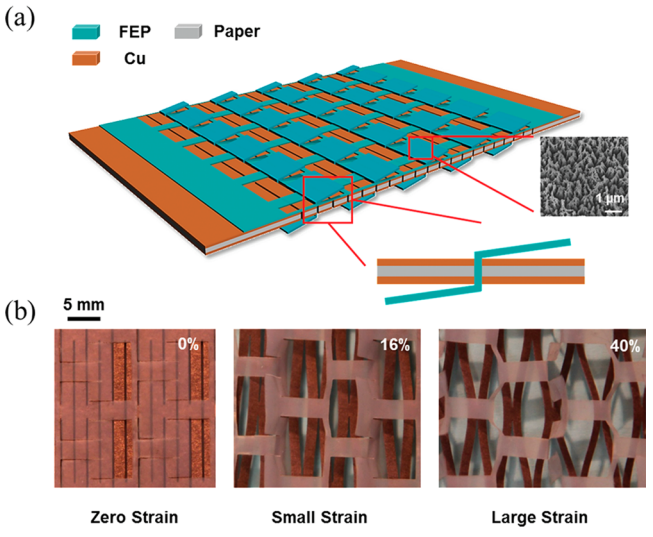

Figure 1. (a) Schematic structure of paper-based K-TENG. The top inset is the SEM image of the FEP film and the bottom inset is the cross-sectional view of the interlocking structure. (b) Photograph of the assembled device under different tensile strains.

copper-coated paper sheet and one FEP thin film interlocked by rationally designed linear and rectangular kirigami patterns (Figure S1). The fabrication process started with laser-cutting a piece of printer paper with the linear kirigami pattern, which has been proven to be a simple but effective method of introducing super high stretchability into stiff sheets. The deformation mechanics and relationship between the unit cell parameters (denoted by horizontal spacing x, vertical spacing y, and cut length l as illustrated in Figure S1) and attainable strain have been well studied.[21] In this work, both the horizontal and vertical spacing between notches were set to be 2 mm, and the cut length was 22 mm. The resulted paper can withstand a tensile strain up to 200% without breaking. Then, copper thin film was sputter-coated onto both sides of the laser-cut paper to serve as one of the triboelectric materials and the electrode of the TENG. FEP thin film with nanowire structures created on both sides through inductively coupled plasma (ICP) to enhance the surface charge density[27−31] was chosen as the other triboelectric material and laser-cut with the rectangular kirigami pattern, whose unit cell parameters were designed to match those of the linear kirigami on paper so that an interlocking structure could be formed. Two rectangles can fit into a single notch of the linear kirigami as shown in Figure S1c. Finally, the prepared FEP film and paper were assembled together to obtain the final device. The effective dimensions of the device were approximately 7.2 cm in length, 6 cm in width, and 150 μm in thickness.

The KTENG operates on the basis of the single-electrode mode,[32,33] and its working principles under stretching operations are illustrated in Figure 2. At the initial state, the copper electrode and FEP film are in contact and there is no electrical output. Due to different surface electron affinities, however, the electrons will be transferred from the copper electrode surface to the FEP surface, leaving net positive charges on the electrode surface and net negative charges on the FEP surface. When a tensile force is applied on the KTENG, the paper and FEP film undergo deformation of different amplitudes due to different kirigami patterns. The rectangular cuts of the FEP film will deflect more from the horizontal surface, and thus, the distance between the copper electrode and FEP will increase. As a result, the charge separation will induce potential difference between the electrode and the ground in the open-circuit condition, and electrons will be driven from the ground to the electrode in the short-circuit condition. As the tensile strain increases and the angular deflection of the rectangular cuts of FEP film reaches approximately 90°, the largest distance between the triboelectric layers as well as the maximum open-circuit potential difference will be achieved, which is defined as the fully stretched state. As the tensile strain continues to increase, the KTENG will transit to overstretched state. The distance between the triboelectric layers and the open-circuit potential difference will start to decrease, and the electrons will flow from the electrode to the ground in the short-circuit condition until the stretching stops. When the tensile force is released and the device recovers to its original state, the distance between the triboelectric layers will increase first until back to the fully stretched state and decrease afterward until back to the initial state, and so is the open-circuit potential difference between the electrode and the ground. In the short-circuit condition, the electrons will first flow from the ground to the electrode before reverting back to the fully stretched state and *vice versa* afterward. Therefore, a cyclic AC output can be generated across the load between the electrode and the ground when a periodic tensile force is applied on the KTENG. In the case that the maximum strain is not large enough, the entire power generation cycle may be partially fulfilled, as illustrated by the dark blue and purple dash lines in Figure 2. The rationally designed interlocking kirigami structure poses restraints on the deformation of FEP film and ensures that the device can recover to its original state when the tensile force is released, which greatly enhances the robustness and reliability of the

DOI: 10.1021/acsnano.6b00949
ACS Nano XXXX, XXX, XXX−XXX

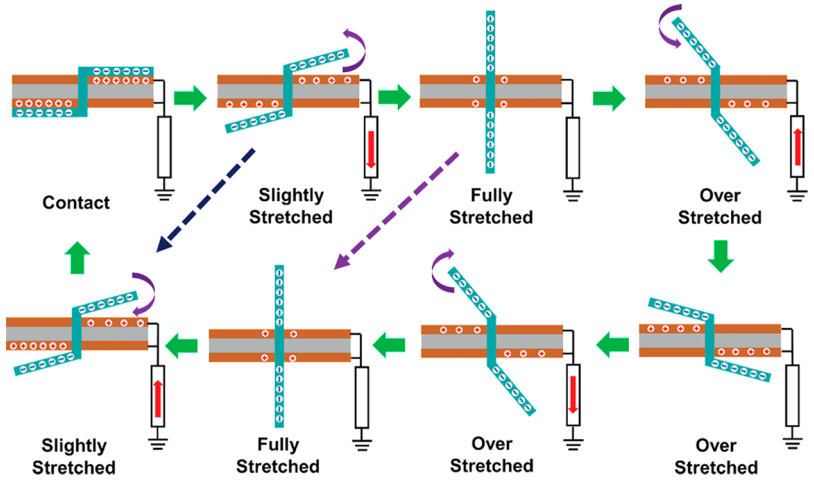

Figure 2. Working mechanism of the K-TENG.

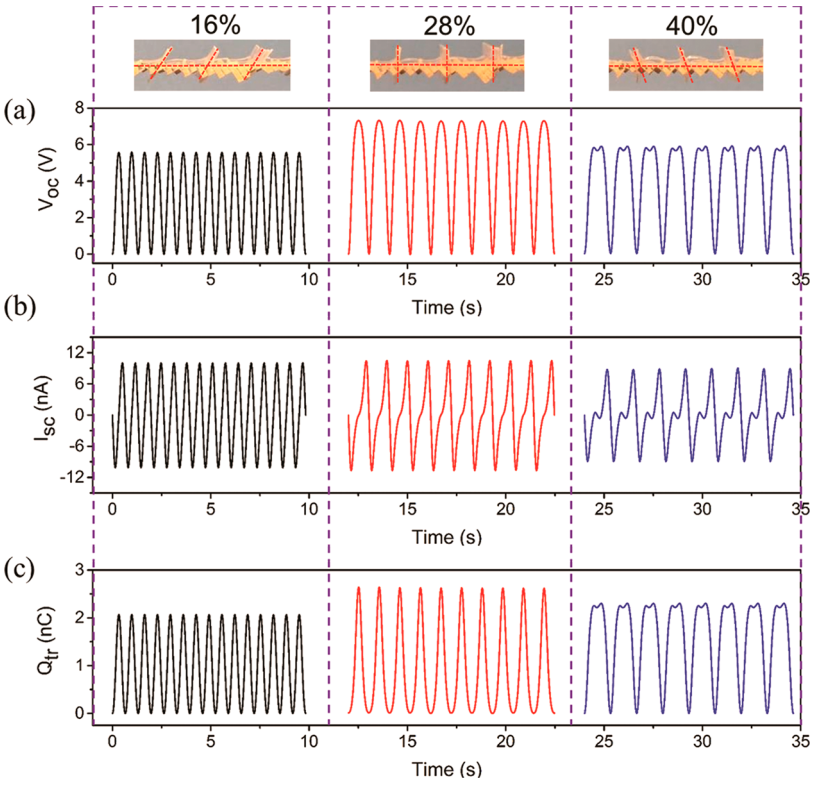

Figure 3. Typical electrical outputs of the paper-based K-TENG at specific stretched strains of 16%, 28%, and 40%. (a) The open-circuit voltage (V_{oc}), (b) the short-circuit current (I_{sc}), and (c) the transferred charge quantity (Q_{tr}). The top insets are the cross-sectional images of the K-TENG under these strains.

device. Furthermore, unlike conventional TENGs which require additional spacers for the charge separation process, the KTENG relies on the deformation of different kirigami structures to induce charge separation. Therefore, the most important feature of the KTENG is the structure with interlocking linear and rectangular kirigami patterns, which not only provides the stretchability and robustness of the device, but also helps to facilitate the charge separation process.

The typical electrical output of the KTENG under cyclic stretching up to specific tensile strains of 16%, 28%, and 40% are plotted in Figure 3. Figure 3a–c presents the open-circuit voltage (V_{oc}), the short-circuit current (I_{sc}) and the transferred charge quantity (Q_{tr}), respectively. The top insets show the cross-sectional photographs of the KTENG at these strains, indicating their differences in deflection magnitude. It can be observed that at the strain of 16%, 28%, and 40%, the device reaches approximately the slightly stretched, fully stretched, and overstretched state, respectively. Therefore, the plotted results can be regarded as the representative data of the output performance when the KTENG is stretched to these states. In the case that the device at the maximum applied strain is at the slightly or fully stretched state, the V_{oc} and Q_{tr} increase monotonically with the applied strain, while the I_{sc} only changes sign at the maximum applied strain and the zero strain. In the case that the device at the maximum applied strain is at the overstretched state, the V_{oc} and Q_{tr} increase first with the

DOI: 10.1021/acsnano.6b00949
ACS Nano XXXX, XXX, XXX–XXX

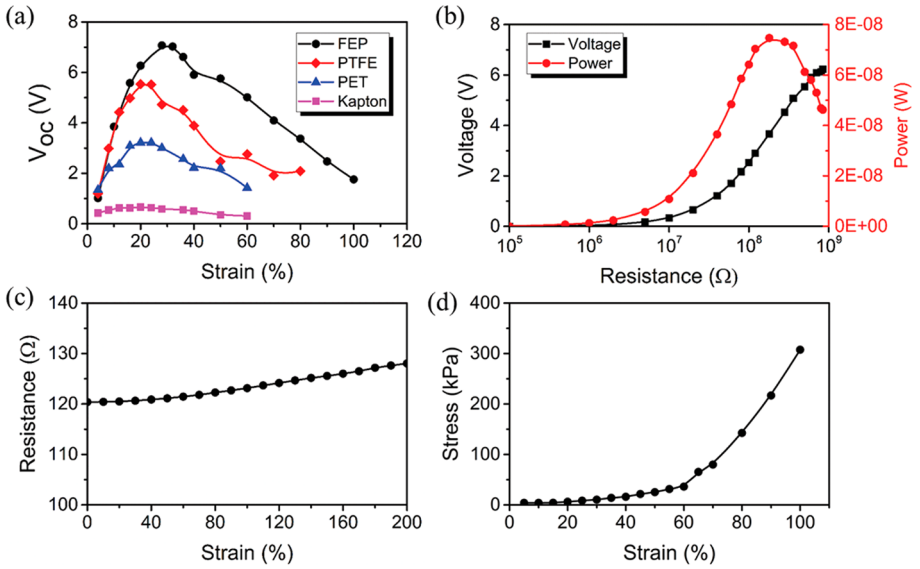

Figure 4. Characteristics of the paper-based FEP K-TENG *vs* stretched strain. (a) The summarized relationship between the V_{oc} and the stretched strain of different materials. (b) Relationship between instantaneous power density and the resistance of external load under 28% strain. (c) Relationship between the resistance of copper-coated kirigami paper and stretched strain. (d) The stress−strain response of the paper-based K-TENG.

applied strain until the strain of the fully stretched state is reached, after which both start to decrease until the maximum applied strain. In the process of recovering to the original zero-strain state, the V_{oc} and Q_{tr} increase again as the device approaches the fully stretched state and start to decrease thereafter. The behavior is clearly reflected by the concave top of the V_{oc} and Q_{tr} plots. Correspondingly, the I_{sc} changes sign not only at the maximum applied strain and the zero strain but also at the strain of the fully stretched state, which results in the small humps at the middle of the I_{sc} plot. The different behaviors of the electrical output when the KTENG is stretched to different states can be well explained by the working principles proposed in Figure 2. In the first two cases of slightly and fully stretched states, the charge separation distance increases monotonically with the applied strain, and thus, the V_{oc} and Q_{tr} change monotonically as well. In the case of overstretched state, the charge separation distance first increases with the applied strain but starts to decrease after the device reaches the fully stretched state, which results in a local maximum of the V_{oc} at the strain of the fully stretched state and an additional position for the sign change of the I_{sc} besides the maximum applied strain and the zero strain. Therefore, the V_{oc} and Q_{tr} will go through the trend of up-down-up-down in one stretch-release cycle as illustrated in Figure 3. It can also be observed that at the strain of the fully stretched state, 28% for the fabricated device, the maximum values obtained for V_{oc}, I_{sc}, and Q_{tr} are approximately 7.32 V, 2.64 nC, and 10.58 nA.

To further evaluate the output performance of the KTENG consisted of Cu-coated paper and FEP film, its V_{oc} when stretched up to different strains is measured and plotted using black lines in Figure 4a. The V_{oc} reaches its maximum when the maximum strain applied is 28%, at which point the device is approximately at the fully stretched state. To demonstrate the versatility of the proposed interlocking kirigami structure for fabricating stretchable TENG, other materials commonly used as triboelectric layers such as PTFE, PET, and Kapton were explored as well. Their thin films were laser cut with the same rectangular kirigami pattern as on the FEP film, and then assembled with the same Cu-coated paper with the linear kirigami pattern. All of these materials are considered as nonstretchable, but the assembled KTENGs can be stretched at least up to a 60% strain. As expected, the material with the best ability to attract electrons, FEP, gives the highest V_{oc}, followed by PTFE and PET. The Kapton KTENG has the lowest output even though it is supposed to have higher ability to attract electrons than PET, according to the summarized triboelectric series. The contradictory experimental result over theoretical expectation can be explained by the high stiffness of Kapton, which makes the Kapton film not able to form intimate contact with the Cu-coated paper after interlocking assembly. Without intimate contact between the triboelectric layers, the transferred charge quantity will be limited, and so is the generated V_{oc}. The maximum tensile strain the devices can withstand is highly dependent on the design parameters of the interlocking kirigami patterns, and their detailed relationship will be the subject of future work.

To evaluate the effective output power of the FEP KTENG, the output voltage was recorded with various resistances applied as the external load. Then, the effective output power of the KTENG was calculated as $P = V^2/R$, where V is the output voltage across the applied load and R is the applied load resistance, and the relationship between the output voltage/power and the resistance was plotted in Figure 4b. As expected, the output voltage of the KTENG was close to zero at the low-resistance region (when load resistance was smaller than 1 MΩ) but increased dramatically as the load resistance kept increasing. The output power initially increased with the load resistance but started to decrease after the resistance reached a certain value. Here, the maximum output power of 74.66 nW was achieved at a load resistance of 180 MΩ.

One critical challenge of fabricating stretchable TENGs is to make stretchable electrodes. To validate the functionality of the stretchable Cu-paper with the linear kirigami pattern, its resistance was recorded at different tensile strains. As seen from Figure 4c, the resistance of the Cu-paper only increased from

DOI: 10.1021/acsnano.6b00949
ACS Nano XXXX, XXX, XXX−XXX

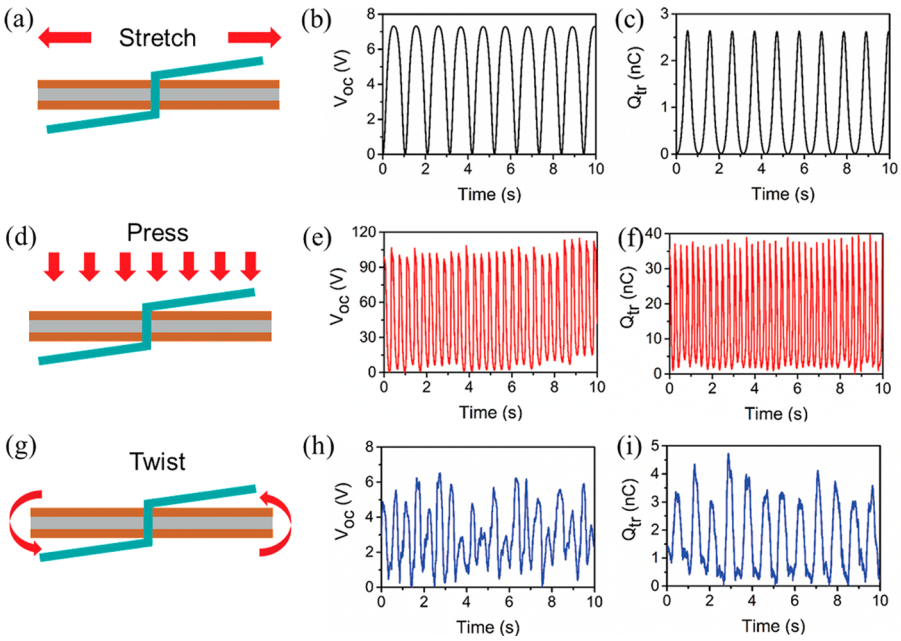

Figure 5. Different operating modes of the paper-based K-TENG. (a–c) KTENG under stretching mode with a 28% strain and its V_{oc} and Q_{tr}. (d–f) KTENG under pressing mode and its V_{oc} and Q_{tr}. (g–i) K-TENG under pressing mode and its V_{oc} and Q_{tr}.

120.39 to 128.03 Ω when the applied strain reached 200%, which is equivalent to a negligible change of 6.34%. This result proves that the linear kirigami pattern is capable of accommodating the applied strain with minimal sacrifice of the conductivity of the stretchable electrode. To characterize the mechanical property of the KTENG, the stresses required for stretching the device to certain strains were measured. It is clear that the KTENG has a two-stage strain–stress response and its tensile modulus of the KTENG experiences a dramatic change from 59.6 to 668.4 kPa when the strain reaches 60%. This phenomenon can be explained by the difference between the structural deformation and material intrinsic deformation. In the first stage, the kirigami patterns render the device stretchable, and thus, the stress required for stretching is mainly attributed to deforming the interlocking kirigami structure, while in the second stage, the FEP film with the rectangular kirigami pattern has reached its limit of structural stretchability, and the FEP material itself undergoes plastic deformation. This is further verified by the stretching limit of a 60% strain for the PET and Kapton KTENG, as shown in Figure 4a. These two materials are stiffer than FEP/PTFE and cannot withstand large tensile strains, which makes the devices consisted of them break once their structural stretching limit from the rectangular kirigami pattern is reached.

As discussed earlier in the working principles of the KTENG under stretching, electrical energy is generated through the distance change between the two triboelectric materials. Any mechanical stimulus that brings about relative motion between the FEP film and the Cu-paper can be converted into electricity. Therefore, the KTENG can be operated under three different modes (stretching, pressing and twisting), and is capable of harvesting energy from various mechanical stimuli, such as pulling, tapping, wind blowing, *etc*. Figure 5 presents the schematics of the KTENG under different operating modes and their typical electrical outputs. The electrical outputs for the stretching mode were recorded when the device was stretched cyclically up to 28%, which yielded a maximum V_{oc} of 7.32 V and a maximum Q_{tr} of 2.64 nC. The pressing mode was demonstrated by hand clapping onto the device, and a maximum V_{oc} of 115.49 V and a maximum Q_{tr} of 39.87 nC were achieved. The twisting mode was realized when the device was held in hands on both ends and twisted repeatedly, with a maximum V_{oc} of 6.55 V and a maximum Q_{tr} of 4.76 nC generated. The stretching and twisting modes had similar maximum output values, but the uniformity of their output profiles as a function of time varied. The stretching outputs were nearly identical for different cycles, while the twisting outputs varied from a cycle to another. As observed from experiments, the KTENG could easily recover back to original interlocking state when the stretching was released, while it was not the case for twisting. The integrity of the rationally designed interlocking structure was prone to damage when the device was twisted and the FEP rectangles tended to pop out from the linear notches on the Cu-paper. The original interlocking state could not be recovered automatically when the twisting force was released, and the resulted interlocking structure was random and usually uneven without perfect position match of the kirigami patterns, which made the outputs nonuniform from cycle to cycle. Fortunately, twisting would not break the materials themselves which were highly flexible owing to the kirigami patterns and their thin-film characteristics, and the rational interlocking design could be easily restored manually. Meanwhile, the outputs of the pressing mode were 1 order of magnitude larger than those of the other two modes, which was attributed to the contact and separation between the hand and the device as well as the more intimate contact between the FEP and the Cu-paper induced when the clapping force was directly applied onto the surface of the device (detailed explanation presented in Figure S2).

The multiple operating modes of the KTENG endow its potential in a broad range of applications. It can be used to power a small LCD screen, light LED arrays, and detect the book opening and closing with no need of external power sources (Supporting Information Figure S3, Movies 1, 2, and 3). In this work, it has also been demonstrated to work as a self-

DOI: 10.1021/acsnano.6b00949
ACS Nano XXXX, XXX, XXX–XXX

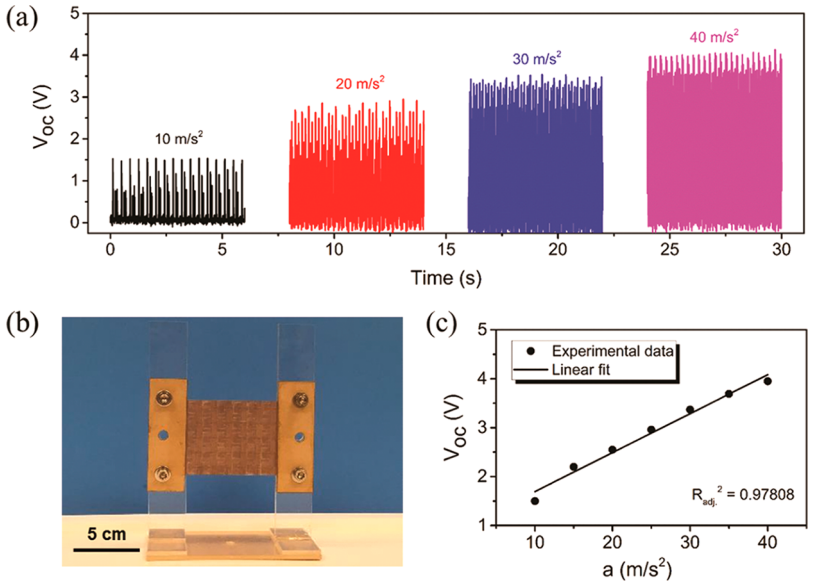

Figure 6. Application of the paper-based K-TENG as a self-powered acceleration sensor. (a) The measured V_{oc} at several specific acceleration rates. (b) Photograph of the acceleration sensor based on the paper-based K-TENG. (c) The summarized relationship between the V_{oc} and the acceleration rates.

powered acceleration sensor. Figure 6a plots its typical outputs at different acceleration/deceleration rates ranging from 10 to 40 m/s^2, and Figure 6b shows the image of the FEP KTENG-based sensor. The two ends of the KTENG are fixed on two beams vertically, and the motion direction is perpendicular to the device plane. The relationship between the maximum V_{oc} and the acceleration rates is summarized in Figure 6c, which clearly suggests a linear dependence with sensitivity of 0.080 V·s^2/m and good sensing performance with a detection range from 10 to 40 m/s^2.

CONCLUSION

In summary, we demonstrated a versatile approach for fabricating highly stretchable, environmentally friendly paper-based TENGs with rationally designed interlocking kirigami structures. The KTENG made of intrinsically inelastic materials could sustain an ultrahigh tensile strain up to 100% and generate maximum outputs of 7.32 V for V_{oc} and 2.64 nC for Q_{tr} with the introduction of kirigami patterns. The interlocking kirigami design not only greatly enhances the rigidity and reliability of the device, but also eliminates the need of additional spacers for the charge separation process as required in conventional TENGs. Owing to its shape-adaptive thin-film design, the KTENG was able to harvest energy from various types of motions (stretching, pressing and twisting). The pressing mode can be easily realized by hand clapping and can generate a maximum V_{oc} of 115.49 V and a maximum Q_{tr} of 39.87 nC. Furthermore, the KTENG has been demonstrated for a broad range of applications, such as powering a LCD screen, lighting LED arrays, self-powered acceleration sensor, and self-powered sensing of book opening and closing. This KTENG work introduces traditional kirigami into the development of stretchable TENGs and verifies its promising applications in both power generation and self-powered sensing.

METHODS

Fabrication of the KTENGs. Ordinary printer paper with a thickness of 100 μm was used as the substrate for the electrode due to its low cost, flexibility and environmental friendliness. The linear kirigami pattern was created using a laser cutter (PLS6.75, Universal Laser Systems) to ensure clean, identical notches. Then, copper was deposited onto the kirigami paper on both sides by magnetron sputtering (PVD75, Kurt J). Thin films of FEP (America Durafilm), PTFE, PET, and Kapton were selected for making the rectangular kirigami structure and all had a thickness of 50 μm. Polymer nanostructures were created on these thin films using ICP after a 10 nm thick gold thin film was deposited by sputtering (Unifilm Sputterer) as the mask. Then, the polymer films were laser-cut with the rectangular kirigami pattern and cleaned with isopropyl alcohol and deionized water, followed by blow drying with nitrogen gas. Finally, the Cu-paper and thin films were assembled together by manually inserting every other row of small rectangles into the linear notches to obtain the KTENGs. Extra space was spared on the two ends to adhere the paper and thin films together using double-sided tape for easy manipulation. The detailed geometry of the Cu-paper and thin films with kirigami patterns was illustrated in Figure S1.

Fabrication of the Self-Powered Acceleration Sensor. The self-powered acceleration sensor consisted of the KTENG and a vertical holder. The holder was made of 1/8 in.-thick acrylic sheets shaped *via* laser cutting. The whole device was secured onto a commercial linear mechanical motor, whose motion was controlled to simulate the acceleration and deceleration processes.

Fabrication of the Self-Powered Sensor for the Detection of Book Opening and Closing. The self-powered sensor for the detection of book opening and closing was miniaturized to have an effective size of 2.4 cm width by 1.2 cm length. It was placed close to the book spine to make it hardly visible without full opening, and its two ends were adhered to two different pages using double-sided tape (as shown in Movie 3).

Characterization. For the measurement of the electric outputs of the KTENG under stretching, one end of the device was fixed on a stationary *XYZ* linear translation stage (462-XYZ-M, Newport Inc.), and the other end was bonded to a linear motor which provides cyclic tensile strains. The open-circuit voltage, transferred charge density, and short-circuit current were measured by a Keithley 6514 system electrometer. The resistance of the as-fabricated Cu-paper was measured by an Amprobe 15XP-B digital multimeter. For the

DOI: 10.1021/acsnano.6b00949
ACS Nano XXXX, XXX, XXX−XXX

measurement of the stress−strain response of the KTENG, one end was fixed on the stationary stage and the other end was secured on a force senor (DFS-BTA, Vernier Software & Technology, LLC) attached to the linear motor. The forces required for different strains controlled by the linear motor were recorded and then divided by the cross-sectional area of the device to obtain corresponding stresses.

ASSOCIATED CONTENT

Supporting Information

The Supporting Information is available free of charge on the ACS Publications website at DOI: 10.1021/acsnano.6b00949.

Figure S1: Kirigami designs. Figure S2: The open-circuit voltage of the FEP K-TENG device under indirect pressing mode. Figure S3: Design of book motion sensor, image and its output screenshots. Figure S4: The open-circuit voltage of the FEP K-TENG device under cyclic stretching at 28% strain before and after 10 000 cycles (PDF)

Movie 1: The application of the paper-based K-TENG for powering a small LCD screen (AVI)

Movie 2: The application of the paper-based K-TENG for powering LED lights (AVI)

Movie 3: The application of the paper-based K-TENG for detection of book opening and closing (AVI)

AUTHOR INFORMATION

Corresponding Author

*E-mail: zlwang@gatech.edu.

Author Contributions

‡C.W. and X.W. contributed equally.

Notes

The authors declare no competing financial interest.

ACKNOWLEDGMENTS

Research was supported by the National Science Foundation (DMR-1505319), the Hightower Chair foundation, and the "thousands talents" program for pioneer researcher and his innovation team, China, National Natural Science Foundation of China (Grant Nos. 51432005, 5151101243, 51561145021).

REFERENCES

(1) Chortos, A.; Bao, Z. Skin-inspired Electronic Devices. *Mater. Today* **2014**, *17*, 321−331.

(2) Yamada, T.; Hayamizu, Y.; Yamamoto, Y.; Yomogida, Y.; Izadi-Najafabadi, A.; Futaba, D. N.; Hata, K. A Stretchable Carbon Nanotube Strain Sensor for Human-Motion Detection. *Nat. Nanotechnol.* **2011**, *6*, 296−301.

(3) Sekitani, T.; Nakajima, H.; Maeda, H.; Fukushima, T.; Aida, T.; Hata, K.; Someya, T. Stretchable Active-Matrix Organic Light-Emitting Diode Display Using Printable Elastic Conductors. *Nat. Mater.* **2009**, *8*, 494−499.

(4) Kim, D.-H.; Ahn, J.-H.; Choi, W. M.; Kim, H.-S.; Kim, T.-H.; Song, J.; Huang, Y. Y.; Liu, Z.; Lu, C.; Rogers, J. A. Stretchable and Foldable Silicon Integrated Circuits. *Science* **2008**, *320*, 507−511.

(5) Xu, L.; Gutbrod, S. R.; Bonifas, A. P.; Su, Y.; Sulkin, M. S.; Lu, N.; Chung, H.-J.; Jang, K.-I.; Liu, Z.; Ying, M.; et al. 3D Multifunctional Integumentary Membranes for Spatiotemporal Cardiac Measurements and Stimulation Across the Entire Epicardium. *Nat. Commun.* **2014**, *5*, 3329.

(6) Xie, K.; Wei, B. Materials and Structures for Stretchable Energy Storage and Conversion Devices. *Adv. Mater.* **2014**, *26*, 3592−3617.

(7) Pushparaj, V. L.; Shaijumon, M. M.; Kumar, A.; Murugesan, S.; Ci, L.; Vajtai, R.; Linhardt, R. J.; Nalamasu, O.; Ajayan, P. M. Flexible Energy Storage Devices Based on Nanocomposite Paper. *Proc. Natl. Acad. Sci. U. S. A.* **2007**, *104*, 13574−13577.

(8) Scrosati, B. Nanomaterials: Paper Powers Battery Breakthrough. *Nat. Nanotechnol.* **2007**, *2*, 598−599.

(9) Gao, K.; Shao, Z.; Wu, X.; Wang, X.; Zhang, Y.; Wang, W.; Wang, F. Paper-Based Transparent Flexible Thin Film Supercapacitors. *Nanoscale* **2013**, *5*, 5307−5311.

(10) Koo, M.; Park, K.-I.; Lee, S. H.; Suh, M.; Jeon, D. Y.; Choi, J. W.; Kang, K.; Lee, K. J. Bendable Inorganic Thin-Film Battery for Fully Flexible Electronic Systems. *Nano Lett.* **2012**, *12*, 4810−4816.

(11) Hu, L.; Pasta, M.; Mantia, F. L.; Cui, L.; Jeong, S.; Deshazer, H. D.; Choi, J. W.; Han, S. M.; Cui, Y. Stretchable, Porous, and Conductive Energy Textiles. *Nano Lett.* **2010**, *10*, 708−714.

(12) Xu, S.; Zhang, Y.; Cho, J.; Lee, J.; Huang, X.; Jia, L.; Fan, J. A.; Su, Y.; Su, J.; Zhang, H.; et al. Stretchable Batteries with Self-similar Serpentine Interconnects and Integrated Wireless Recharging Systems. *Nat. Commun.* **2013**, *4*, 1543.

(13) Wang, Z. L. Triboelectric Nanogenerators as New Energy Technology for Self-Powered Systems and as Active Mechanical and Chemical Sensors. *ACS Nano* **2013**, *7*, 9533−9557.

(14) Fan, F.-R.; Tian, Z.-Q.; Lin Wang, Z. Flexible Triboelectric Generator. *Nano Energy* **2012**, *1*, 328−334.

(15) Wang, Z. L.; Chen, J.; Lin, L. Progress in Triboelectric Nanogenerators as a New Energy Technology and Self-powered Sensors. *Energy Environ. Sci.* **2015**, *8*, 2250−2282.

(16) Guo, H.; Leng, Q.; He, X.; Wang, M.; Chen, J.; Hu, C.; Xi, Y. A Triboelectric Generator Based on Checker-Like Interdigital Electrodes with a Sandwiched PET Thin Film for Harvesting Sliding Energy in All Directions. *Adv. Energy Mater.* **2015**, *5*, 1400790.

(17) Hinchet, R.; Seung, W.; Kim, S.-W. Recent Progress on Flexible Triboelectric Nanogenerators for SelfPowered Electronics. *ChemSusChem* **2015**, *8*, 2327−2344.

(18) Yang, P.-K.; Lin, L.; Yi, F.; Li, X.; Pradel, K. C.; Zi, Y.; Wu, C.-I.; He, J.-H.; Zhang, Y.; Wang, Z. L. A Flexible, Stretchable and Shape-Adaptive Approach for Versatile Energy Conversion and Self-Powered Biomedical Monitoring. *Adv. Mater.* **2015**, *27*, 3817−3824.

(19) Yi, F.; Lin, L.; Niu, S.; Yang, P. K.; Wang, Z.; Chen, J.; Zhou, Y.; Zi, Y.; Wang, J.; Liao, Q.; Zhang, Y.; Wang, Z. L. Stretchable-Rubber-Based Triboelectric Nanogenerator and Its Application as Self-Powered Body Motion Sensors. *Adv. Funct. Mater.* **2015**, *25*, 3688−3696.

(20) Hwang, B.-U.; Lee, J.-H.; Trung, T. Q.; Roh, E.; Kim, D.-I.; Kim, S.-W.; Lee, N.-E. Transparent Stretchable Self-Powered Patchable Sensor Platform with Ultrasensitive Recognition of Human Activities. *ACS Nano* **2015**, *9*, 8801−8810.

(21) Shyu, T. C.; Damasceno, P. F.; Dodd, P. M.; Lamoureux, A.; Xu, L.; Shlian, M.; Shtein, M.; Glotzer, S. C.; Kotov, N. A. A Kirigami Approach to Engineering Elasticity in Nanocomposites Through Patterned Defects. *Nat. Mater.* **2015**, *14*, 785−789.

(22) Lamoureux, A.; Lee, K.; Shlian, M.; Forrest, S. R.; Shtein, M. Dynamic Kirigami Structures for Integrated Solar Tracking. *Nat. Commun.* **2015**, *6*, 8092.

(23) Song, Z.; Ma, T.; Tang, R.; Cheng, Q.; Wang, X.; Krishnaraju, D.; Panat, R.; Chan, C. K.; Yu, H.; Jiang, H. Origami Lithium-ion Batteries. *Nat. Commun.* **2014**, *5*, 3140.

(24) Silverberg, J. L.; Evans, A. A.; McLeod, L.; Hayward, R. C.; Hull, T.; Santangelo, C. D.; Cohen, I. Using Origami Design Principles to Fold Reprogrammable Mechanical Metamaterials. *Science* **2014**, *345*, 647−650.

(25) Cho, J.-H.; Keung, M. D.; Verellen, N.; Lagae, L.; Moshchalkov, V. V.; Van Dorpe, P.; Gracias, D. H. Nanoscale Origami for 3D Optics. *Small* **2011**, *7* (14), 1943−1948.

(26) Yang, P.-K.; Lin, Z.-H.; Pradel, K. C.; Lin, L.; Li, X.; Wen, X.; He, J.-H.; Wang, Z. L. Paper-Based Origami Triboelectric Nanogenerators and Self-Powered Pressure Sensors. *ACS Nano* **2015**, *9*, 901−907.

(27) Yeh, M.-H.; Lin, L.; Yang, P.-K.; Wang, Z. L. Motion-Driven Electrochromic Reactions for Self-Powered Smart Window System. *ACS Nano* **2015**, *9*, 4757−4765.

DOI: 10.1021/acsnano.6b00949
ACS Nano XXXX, XXX, XXX−XXX

(28) Jeong, C. K.; Baek, K. M.; Niu, S.; Nam, T. W.; Hur, Y. H.; Park, D. Y.; Hwang, G.-T.; Byun, M.; Wang, Z. L.; Jung, Y. S.; Lee, K. J. Topographically-Designed Triboelectric Nanogenerator *via* Block Copolymer Self-Assembly. *Nano Lett.* **2014**, *14*, 7031−7038.
(29) Lin, L.; Xie, Y.; Niu, S.; Wang, S.; Yang, P.-K.; Wang, Z. L. Robust Triboelectric Nanogenerator Based on Rolling Electrification and Electrostatic Induction at an Instantaneous Energy Conversion Efficiency of ∼ 55%. *ACS Nano* **2015**, *9*, 922−930.
(30) Xie, Y.; Wang, S.; Niu, S.; Lin, L.; Jing, Q.; Yang, J.; Wu, Z.; Wang, Z. L. Grating-Structured Freestanding Triboelectric-Layer Nanogenerator for Harvesting Mechanical Energy at 85% Total Conversion Efficiency. *Adv. Mater.* **2014**, *26*, 6599−6607.
(31) Fang, H.; Wu, W.; Song, J.; Wang, Z. L. Controlled Growth of Aligned Polymer Nanowires. *J. Phys. Chem. C* **2009**, *113*, 16571−16574.
(32) Niu, S.; Liu, Y.; Wang, S.; Lin, L.; Zhou, Y. S.; Hu, Y.; Wang, Z. L. Theoretical Investigation and Structural Optimization of Single-Electrode Triboelectric Nanogenerators. *Adv. Funct. Mater.* **2014**, *24*, 3332−3340.
(33) Yang, Y.; Zhang, H.; Chen, J.; Jing, Q.; Zhou, Y. S.; Wen, X.; Wang, Z. L. Single-Electrode-Based Sliding Triboelectric Nanogenerator for Self-Powered Displacement Vector Sensor System. *ACS Nano* **2013**, *7*, 7342−7351.

DOI: 10.1021/acsnano.6b00949
ACS Nano XXXX, XXX, XXX−XXX